Analysis of Beat Noise in Coherent and Incoherent Time-Spreading OCDMA

Xu Wang, *Member, IEEE,* and Ken-ichi Kitayama, *Fellow, IEEE*

***Abstract*—The effect of beat noise and other types of additive noise in time-spreading optical-code-division multiple-access (TS-OCDMA) networks is analyzed in this paper. By defining the coherent ratio kt, the ratio of the chip duration to the coherence time of the light source, TS-OCDMA systems are classified into incoherent, partially coherent, and coherent systems. The noise distributions and the bit-error rates are derived, and system performance is discussed for different cases. The performance of coherent systems is limited by the beat noise. With increasing kt, the effect of beat noise decreases in incoherent systems, and they eventually become free of beat noise. Possible solutions to the beat noise problem in coherent and partially coherent systems are also proposed and discussed.**

***Index Terms*—Beat noise, code-division multiple access (CDMA), communication systems, optical networks.**

I. Introduction

IT is well known that the most critical segment of any telecommunication network is the last mile because it provides the link to the business or residential customers who provide revenues. The next-generation last-mile (or access) network, which will deliver various next-generation services (Ethernet, video, and voice) all at the same time, is expected to be a new driving force for telecommunications. Only optical techniques, passive optical networks (PONs) in particular, can provide sufficient bandwidth for this requirement. Existing optical access techniques for this purpose include time-division multiple access (TDMA), wavelength-division multiple access (WDMA), subcarrier multiple access (SCMA), and code-division multiple access (CDMA).

Optical CDMA (OCDMA), where different users are assigned different codes during transmission, is a promising candidate for next-generation broad-band access networks. It offers several unique advantages [1]–[6].

1) *All optical processing*: Unlike wireless CDMA, coding operations are performed all optically in OCDMA, as is desirable for the PON requirement.
2) *Fully asynchronous transmission*: The OCDMA network can work with fully asynchronous transmission without requiring complex and expensive electronic equipment and protocols.
3) *Low-delay access*: OCDMA enables a low access delay as the coding operations are performed all optically and passively.
4) *Soft capacity on demand*: Users can be easily added or removed as demand changes.
5) *Potential security*: High security can be ensured by using long pseudorandom codes for transmission.
6) *Quality of service control*: The quality of service (QoS) can be easily controlled in physical layer by assigning different codes indicating the appropriate QoS to users.

Generally, OCDMA techniques can be classified based on two criteria. First, based on the working principle, OCDMA can be classified into *incoherent* OCDMA [1]–[10], where coding is done on an optical power basis, and *coherent* OCDMA [3]–[6], [11]–[13], where the coding is done on a field amplitude basis. Second, based on coding dimensions, OCDMA coding operations can be one-dimensional (1-D) to be performed in either the *time* domain [1]–[7], [11]–[13] or the *frequency* domain [8]–[10], [14]–[17] or be two-dimensional (2-D) to be performed in the *frequency* and *time* domains simultaneously [18]–[25].

Incoherent time-spreading (TS) OCDMA has been studied for a long time because it is easy to be implemented at a relatively low bit rate [1]–[9]. The coding operation is performed in a unipolar (0, 1) manner because of the incoherence. This leads to several disadvantages, such as a small code size, low power and bandwidth efficiency, and poor correlation [1]–[4]. Several schemes have been proposed to overcome this issue electrically [7]–[10], but these suffer from the optoelectronic bandwidth bottleneck. Coding in the frequency domain (especially with 2-D schemes) provides a new freedom and will result in better correlation performance by using more frequency resources [18]–[25]; however, it will also suffer from the dispersion problem, which is not easily solved in such a broad-band application.

Coherent OCDMA is superior to incoherent schemes in overall performance because coding operations are performed in a bipolar (-1, $+1$) manner in the optical domain [3]–[6], [11]–[14]. Among the coherent schemes proposed so far, coherent TS OCDMA is the most desirable choice for practical use in terms of the correlation property, frequency efficiency, and dispersion [4]–[6], [11], [12], [26], [27]. However, the optical path of the encoder/decoder must be controlled within an optical wavelength order. Previously, only planar lightwave circuits (PLCs) have been used for this purpose [4]–[6]. Unfortunately, the PLC is not a practical choice so far in terms of cost, volume, insertion loss, or compatibility with the fiber-optic system. Recently, superstructure fiber Bragg grating (SSFBG)

Manuscript received June 24, 2003; revised June 7, 2004.

X. Wang was with the Department of Electronics and Information Systems, Osaka University, Osaka 565-0871, Japan. He is now with the Ultra-fast Photonic Network Group, Information and Network System Division, National Institute of Information and Communication Technology (NICT), Tokyo 184-8795, Japan (e-mail: xwang@nict.go.jp).

K. Kitayama is with the Department of Electronics and Information Systems, Graduate School of Engineering, Osaka University, Osaka 565-0871, Japan.

Digital Object Identifier 10.1109/JLT.2004.833267

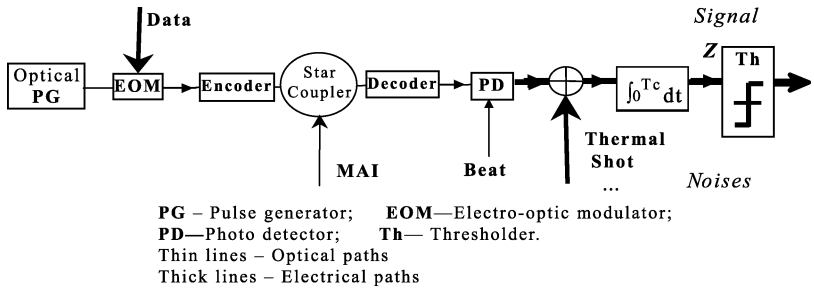

Fig. 1. System model of the OCDMA-PON and noise sources.

has been reported that offers high performance, compactness, compatibility with the fiber-optic system, and potentially low cost, making it an attractive choice for coherent TS-OCDMA encoding/decoding [26], [27]. The improved practically of coherent TS-OCDMA has attracted a great deal of research attention.

In coherent TS-OCDMA, the coherence of the optical signal has to be maintained within the chip duration so the coherent beat noise becomes critical. The beat noise issue has been studied with respect to spectral coding OCDMA systems [10], [28] and 2-D OCDMA [29]. The effect of beat noise in a TS-OCDMA system, however, has not been studied to the authors' knowledge. This paper examines the beat noise, along with the multiple-access-interference (MAI) and receiver noise, and the effects of such noise on incoherent, coherent, and partially coherent TS-OCDMA.

This paper is organized as follows. In Section II, the system models of coherent, incoherent, and partially coherent TS-OCDMA-PON that were used are described. The noise distributions and corresponding bit-error-rate (BER) expressions are derived and discussed in Section III. In Section IV, the system performance of these networks and the effect of the beat noise are evaluated and possible solutions discussed. Conclusions are presented in Section V.

II. System Model

A simplified system model of a TS-OCDMA-PON is shown in Fig. 1. Three different kinds of noise source should be taken into account in this model: MAI noise arising from the network, beat noise at the detector, and receiver noise (thermal, shot noise, etc.). The bandwidth of the receiver is limited to the chip rate and thus is equivalent to an integrator (over one-chip interval) followed by thresholding [2], [7].

We assume that there are K active users asynchronously transmitting signals in the network. If there are $m\,(0 < m < K)$ interfering signals from untargeted active users at a given instant, the received optical field at the photodetector of the target user is

$$E(t) = \sqrt{P_d}\exp j\left(\omega_d \cdot t + \phi_d(t)\right) + \sum_{i=1}^{m}\sqrt{P_i}\exp j\left(\omega_i \cdot (t-\tau_i) + \phi_i(t-\tau_i)\right) \quad (1)$$

where P_d and P_i are the optical intensity of the decoded signal from the targeted (data) and untargeted users (interferers), respectively, ω_d and ω_i are optical frequencies, ϕ_d and ϕ_i are the respective phase noise of these signals, and τ_i is the relative network transit delay of the interferer. We assume that ϕ_d and ϕ_i are mutually independent Gaussian-distributed Wiener–Levy stochastic processes [30]–[32].

For a TS-OCDMA network employing chip-rate square-low photodetection, the output signal Z from the integrator is

$$\begin{aligned} Z &= \int_0^{T_c} \Re\cdot(E\cdot E^*)dt + \int_0^{T_c} n_0(t)dt \\ &= \underbrace{T_c\Re P_d}_{\text{Data}} + \underbrace{T_c\Re\sum_{i=1}^{m}P_i + 2\Re\sum_{i=1}^{m}\sqrt{P_dP_i}}_{\text{Interference}} \\ &\quad \times \underbrace{\int_0^{T_c}\cos\left((\omega_i-\omega_d)t-\omega_i\tau_i+\phi_i(t-\tau_i)-\phi_d(t)\right)dt}_{\text{Primary data-interference beat terms}} \\ &\quad + 2\Re\sum_{j=i+1}^{m}\sum_{i=1}^{m-1}\sqrt{P_iP_j} \\ &\quad \times \underbrace{\int_0^{T_c}\cos\left((\omega_i-\omega_j)t-\omega_i\tau_i+\omega_j\tau_j+\phi_i(t-\tau_i)\right.}_{\text{Secondary interference-interference beat terms}} \\ &\quad \left.-\phi_j(t-\tau_j)\right)dt + \underbrace{\int_0^{T_c} n_0(t)dt}_{\text{Receiver noise}} \end{aligned} \quad (2)$$

where $\Re$ is the responsivity of the photodetector, T_C is the chip duration, and n_0 denotes the receiver noise current. Here, it is assumed that the bandwidth of photodetector is larger than the frequency difference between the incoming signals $(\omega_i - \omega_d)$. The chip pulse waveform is also assumed to be constant over the chip duration T_c for simplicity. In this expression, the first term is the target signal, the second term represents the MAI noise, and the third and fourth terms are the m primary data–interference and $m(m-1)/2$ secondary interference–interference beat noise, respectively. The final term represents the receiver noise. Here, the polarization states of the data and interfering signals are assumed to be the same (the worst-case scenario).

Usually, in a TS-OCDMA-PON, the crosstalk level ξ, which is defined as $\xi \equiv \langle P_i\rangle/P_d$ (here, $\langle\bullet\rangle$ represents the assemble average), is very small ($\xi \ll 1$). For example, in a coherent TS-CDMA-PON with the SSFBG encoder/decoder using length N_{Chip} Gold code, $\xi \approx 1/N_{\text{Chip}}$. The ratio of the variance of primary and secondary beat noise terms is about $2/(m\sqrt{\xi})$. If

m is not very large ($m\sqrt{\xi} \ll 1$), the secondary beat noise can be ignored. Generally, we can therefore focus on the primary data–interference beat terms. For the case where the secondary beat terms cannot be ignored, the discussion is similar.

In the expression of the primary beat terms (the third sum in (2)), there are three terms inside the cosine functions. The first term is $(\omega_i - \omega_j)\cdot t \equiv (\delta\omega)_{ij}.t$. Typically, we assume $(\delta\omega)_{ij} \leq$ 1 GHz [32] and $T_C \approx 10$ ps [33], [34] in TS-OCDMA, the term $(\delta\omega)_{ij}t \ll 2\pi$ within the integral duration T_C, so the first term is negligible. The second term $\omega_i\tau_i$ is approximately a constant during the integral duration, so this is also a negligible term. The third term $\phi(t-\tau_i) - \phi(t-\tau_j) \equiv \delta\phi_{ij}(t)$ strongly depends on the coherent property of the optical pulse within the integral duration. We will discuss the effects of this term in three different cases: an incoherent regime, a coherent regime, and a partially coherent regime.

A. Incoherent Regime ($\tau_c \ll T_C$)

In incoherent TS-OCDMA, it is usually assumed that $\tau_c \ll T_C$ (τ_c is the coherence time of the light [32]). In this regime, $\delta\phi_{ij}(t)$ is a random process uniformly distributed over $[-\pi, \pi]$ during the integral duration T_C. The integral of the cosine function thus gives 0. We can simplify Z to

$$Z = T_c\Re\left(P_d + \sum_{i=1}^{m} P_i\right) + \int_0^{T_c} n_0(t)dt. \tag{3}$$

This means that the beat noise can be ignored by averaging throughout the detection, and the MAI noise is the dominant noise source in such systems.

B. Coherent Regime ($\tau_c \geq T_C$)

In contrast, in coherent TS-OCDMA (e.g., with PLCs or an SSFBG encoder/decoder), the coherence of light should be maintained at least within each chip; i.e., $\tau_c \geq T_C$. In this regime, $\delta\phi_{ij}(t)$ is a small constant within the integral duration T_C. Thus, Z becomes

$$Z \approx T_c\Re\left(P_d + \sum_{i=1}^{m} P_i\right) + \Re T_c\left[2\sum_{i=1}^{m}\sqrt{P_iP_d}\cos(\Delta\Phi_i)\right] + \int_0^{T_c} n_0(t)dt. \tag{4}$$

Here, we ignore the secondary interference–interference beat noise terms for simplicity. $\Delta\Phi_i \equiv (\delta\omega)_{id}T_C + \omega_i\tau_i + \delta\phi_{id}$ denotes the overall phase noise. $\Delta\Phi_i$ is a random process that varies over $[-\pi, \pi]$ from bit to bit, which results in beat noise in coherent TS-OCDMA systems.

C. Partially Coherent Regime ($T_C/\tau_c > 1$)

Usually, in an incoherent TS-OCDMA network, the ratio T_C/τ_c is not very high. Here, we define the *coherent ratio* $kt \equiv T_C/\tau_c$ to measure the coherence property of the light within the chip duration. As $\tau_c \sim 1/B_o$ (B_o is the optical bandwidth of the system), $kt \sim T_CB_o$. In practice, most incoherent TS-OCDMA systems are partially coherent ($kt > 1$) as T_C is usually very short and B_o cannot be very large. For instance, if $T_C \sim 10$ ps, the coherent ratio kt of a system with 2-nm bandwidth ($B_o \sim 250$ GHz) is only about 2.5. That is far from the incoherent regime. To attain $kt = 10$, an 8-nm bandwidth is required, which is prohibitively large. Therefore, it is important to determine the relationship between the beat noise and the coherent ratio kt of TS-OCDMA systems.

In the partially coherent regime, a simplification of the model is to assume that the relative phase $\Delta\Phi_{in}$ is maintained as a constant within every time slot of coherent time τ_c, and they are mutually independent random processes distributed over $[-\pi, \pi]$ for different time slots. Under this assumption, Z can be expressed as

$$Z \approx T_c\Re\left(P_d + \sum_{i=1}^{m} P_i\right) + \Re\tau_c\sum_{n}^{kt}\left[2\sum_{i=1}^{m}\sqrt{P_iP_d}\cos(\Delta\Phi_{in})\right] + \int_0^{T_c} n_0(t)dt. \tag{5}$$

Within the limit of $kt = 1$, (5) becomes that of the *coherent* regime (i.e., (4)). Within the limit of $kt \to \infty$, (5) becomes that of the *incoherent* regime [i.e., (3)].

III. Noise Distributions and BER Expressions

The average BER of the system can be written as

$$\text{BER} = \sum_{m=0}^{K-1} p(m)\ \text{BER}\ (m) \tag{6}$$

where $p(m)$ is the probability that m of the $K-1$ interfering users are simultaneously "1"s at the detection chip, which obeys the binomial distribution

$$p(m) = \frac{(K-1)!}{(K-m-1)!m!}2^{-(K-1)}. \tag{7}$$

BER(m) is the BER with m interfering signals. With equal probability binary data and chip rate detection, BER(m) can be expressed as

$$\begin{aligned}\text{BER}(m) &= \Pr(0)_{\text{chip}}Pe(1|0)(m) + \Pr(1)_{\text{chip}}Pe(0|1)(m)\\ &= \left[\Pr(0)_{\text{data}} + \Pr(1)_{\text{data}}\left(1 - \frac{T_C}{T_{\text{Bit}}}\right)\right]Pe(1|0)(m)\\ &\quad + \left[\Pr(1)_{\text{data}}\frac{T_C}{T_{\text{Bit}}}\right]Pe(0|1)(m)\\ &= \frac{1}{2}\left[\left(2 - \frac{T_C}{T_{\text{Bit}}}\right)Pe(1|0)(m) + \frac{T_C}{T_{\text{Bit}}}Pe(0|1)(m)\right]\end{aligned} \tag{8}$$

where $\Pr(0)_{\text{chip}}$ and $\Pr(1)_{\text{chip}}$ are the probabilities of chip mark "0" and "1", respectively, while $\Pr(0)_{\text{data}}$ and $\Pr(1)_{\text{data}}$ are the probabilities of data mark "0" and "1", respectively. T_{Bit} is the bit period, and $Pe(1|0)(m)$ and $Pe(0|1)(m)$ are conditional error probabilities with chip mark "0" and "1", respectively.

We can thus discuss the noise distributions from (3)–(5) for different systems and derive BER expressions of them.

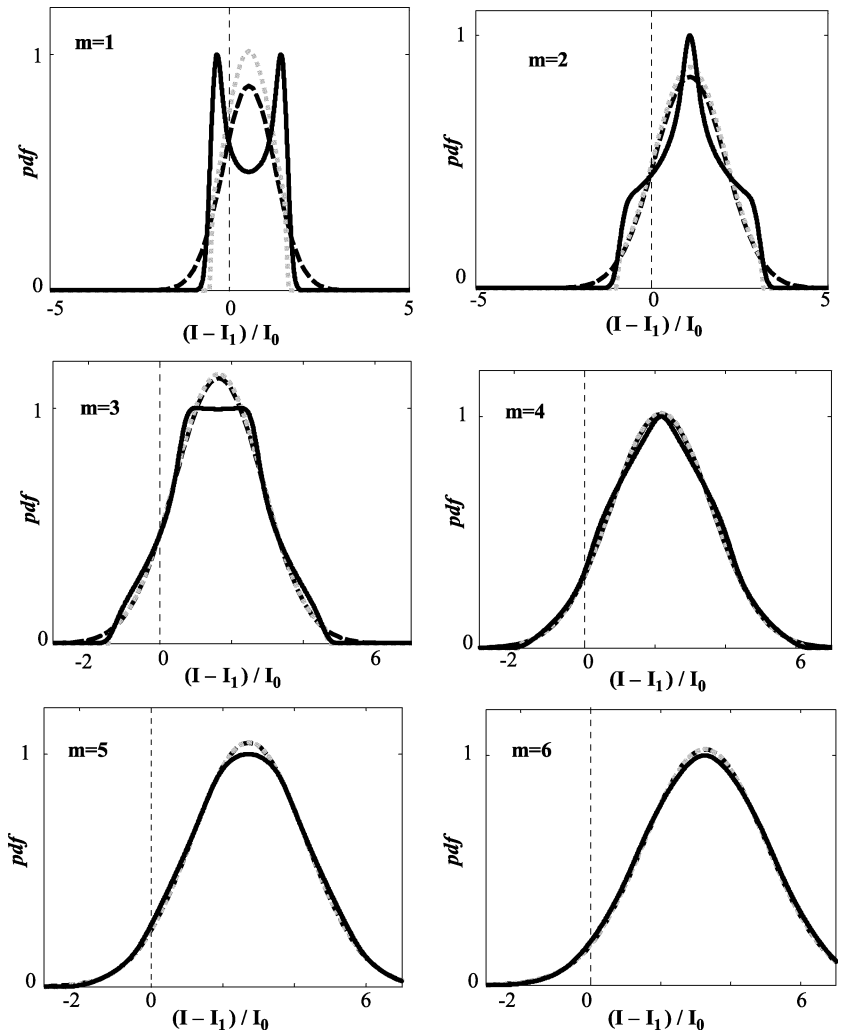

Fig. 2. Noise pdf with different values of m ($I_1 = P_d$, $I_0 = 2\sqrt{\xi P_d}$). Solid black lines: Calculate by (12). Dashed black lines: Gaussian pdf. Dotted gray lines: Modified Gaussian pdf.

A. Incoherent Regime ($kt \to \infty$)

From (3), the average received signal scaled by $1/T_c\Re$ is

$$\frac{\langle Z \rangle}{T_c\Re} = (1 + m\xi)P_d. \tag{9}$$

If we assume that the MAI and receiver noise both have Gaussian distributions, the error probabilities are

$$Pe(1|0)(m) = \frac{1}{2}\mathrm{erfc}\left[\frac{P_d(D - m\xi)}{\sqrt{2}\sigma_{0-\mathrm{in}}}\right] \tag{10a}$$

and

$$Pe(0|1)(m) = \frac{1}{2}\mathrm{erfc}\left[\frac{P_d(1 + m\xi - D)}{\sqrt{2}\sigma_{1-\mathrm{in}}}\right] \tag{10b}$$

where $0 < D < 1 + m\xi$ is the decision threshold. In addition, $\sigma_{0-\mathrm{in}}$ and $\sigma_{1-\mathrm{in}}$ are the total noise variance with chip mark "0" or "1", respectively

$$\begin{aligned}\sigma_{0-\mathrm{in}}^2 &= \sigma_{\mathrm{MAI}}^2 + \sigma_{\mathrm{th}}^2 + \sigma_{0-\mathrm{sh}}^2 \\ \sigma_{1-\mathrm{in}}^2 &= \sigma_{\mathrm{MAI}}^2 + \sigma_{\mathrm{th}}^2 + \sigma_{1-\mathrm{sh}}^2\end{aligned} \tag{11a}$$

where σ_{MAI}, σ_{th}, and σ_{sh} are the MAI, thermal, and shot noise variances, respectively

$$\begin{aligned}\sigma_{\mathrm{MAI}}^2 &= m\sigma_{\mathrm{MAI}-0}^2 \\ \sigma_{\mathrm{th}}^2 &= \frac{4k_BTB_R}{R_L} = B_RN_{\mathrm{th}} \\ \sigma_{0-\mathrm{sh}}^2 &= 2eB_R\Re P_d m\xi \\ \sigma_{1-\mathrm{sh}}^2 &= 2eB_R\Re P_d(1 + m\xi).\end{aligned} \tag{11b}$$

Here, $\sigma_{\mathrm{MAI}-0}$ is the variance of a single interfering signal; when using $N_{\mathrm{Chip}} = 127$ Gold code, $\sigma_{\mathrm{MAI}-0}^2 \approx 6.5 \times 10^{-5}$. $B_R = 1/(2T_C)$ is the receiver bandwidth, and $N_{\mathrm{th}} = 4k_BT/R_L$ is the thermal noise spectral density, where k_B is Boltzman's constant, T is the temperature, and R_L is the load resistance. A typical value of $N_{\mathrm{th}} = 1$ pA^2/Hz is used in the following calculations. e is the electron charge.

B. Coherent Regime ($kt = 1$)

Within this limit, the average received signal scaled by $1/T_c\Re$ is also given by (9). When the chip mark is "0" ($P_d = 0$), and if the secondary beat terms are negligible, $Pe(1|0)(m)$ is also the same as given by (10a). If the number of secondary beat terms is large enough that it is not negligible, it can also be modeled

to have a normal Gaussian distribution according to the central limit theorem. Therefore, $Pe(1|0)(m)$ will have the same form as (10a) with $\sigma_{0-\text{in}}$ replaced by $\sigma_{0-\text{co}}$

$$\sigma_{0-\text{co}}^2 = \sigma_{\text{MAI}}^2 + \sigma_{\text{th}}^2 + \sigma_{\text{beat}-0}^2 \tag{12a}$$

where $\sigma_{\text{beat}-0}$ is the variance of the secondary beat noise

$$\sigma_{\text{beat}-0}^2 = m(m-1)\xi^2 P_d^2. \tag{12b}$$

With chip mark "1", the beat between each interference with the target signal has a "two-pronged" distribution [30]–[32]. The probability density function (pdf) of the total received signal can be expressed as

$$\text{pdf}(x,m) = F\left[M(\omega)\right] = \frac{1}{2\pi}\int_{-\infty}^{\infty} M(\omega)\exp(-j\omega x)d\omega \tag{13a}$$

where $M(\omega)$ is the characteristic function of the signal [32] and is defined as

$$M(\omega) \equiv \int_{-\infty}^{\infty} \exp(-j\omega x)dx. \tag{13b}$$

From (4) and (13b), we can easily derive

$$M(\omega) = J_0^m(2\sqrt{\xi}P_d\omega)\exp\left[-\frac{\sigma_{1-in}^2\omega^2}{2}\right] \times \exp\left[jm(\xi+\sqrt{\xi})P_d\omega\right] \tag{14}$$

where J_0 is the Bessel function of first kind zero order. Thus, the error probability for mark "1" can be expressed as

$$Pe(0|1)(m) = \int_0^{DP_d} \text{pdf}(x,m)dx. \tag{15}$$

We have applied two approximations for this pdf to simplify the calculation [33]. One is to use the Gaussian distribution with $\sigma_{1-\text{co}}$

$$\sigma_{1-\text{co}}^2 = \sigma_{\text{beat}-1}^2 + \sigma_{\text{MAI}}^2 + \sigma_{\text{th}}^2 + \sigma_{1-\text{sh}}^2 \tag{16}$$

where $\sigma_{\text{beat}-1}$ is the variance of the beat noise, which can be expressed as

$$\sigma_{\text{beat}-1}^2 = 2m\xi P_d^2.$$

We can then calculate $Pe(0|1)(m)$ using (10b) by replacing $\sigma_{1-\text{in}}$ with $\sigma_{1-\text{co}}$. According to the central limit theorem, we can expect this approximation to be valid when m is large enough.

When the m value is low, as the pdf of each interferer beat term is two-pronged and bounded within $2\sqrt{\xi}P_d$, we apply another approximation to modify the Gaussian pdf by bounding the beat noise pdf within $2m\sqrt{\xi}P_d$ and replacing it by that without beat noise. The modified Gaussian distribution with variance σ_{1-m} is

$$\sigma_{1-m}^2 = \begin{cases} \sigma_{1-\text{co}}^2 = \sigma_{\text{beat}-1}^2 + \sigma_{\text{MAI}}^2 \\ \qquad + \sigma_{\text{th}}^2 + \sigma_{1-\text{sh}}^2, & \text{if } D > 1 + m\xi - 2m\sqrt{\xi} \\ \sigma_{1-\text{in}}^2 = \sigma_{\text{MAI}}^2 + \sigma_{\text{th}}^2 \\ \qquad + \sigma_{1-\text{sh}}^2, & \text{others} \end{cases}. \tag{17a}$$

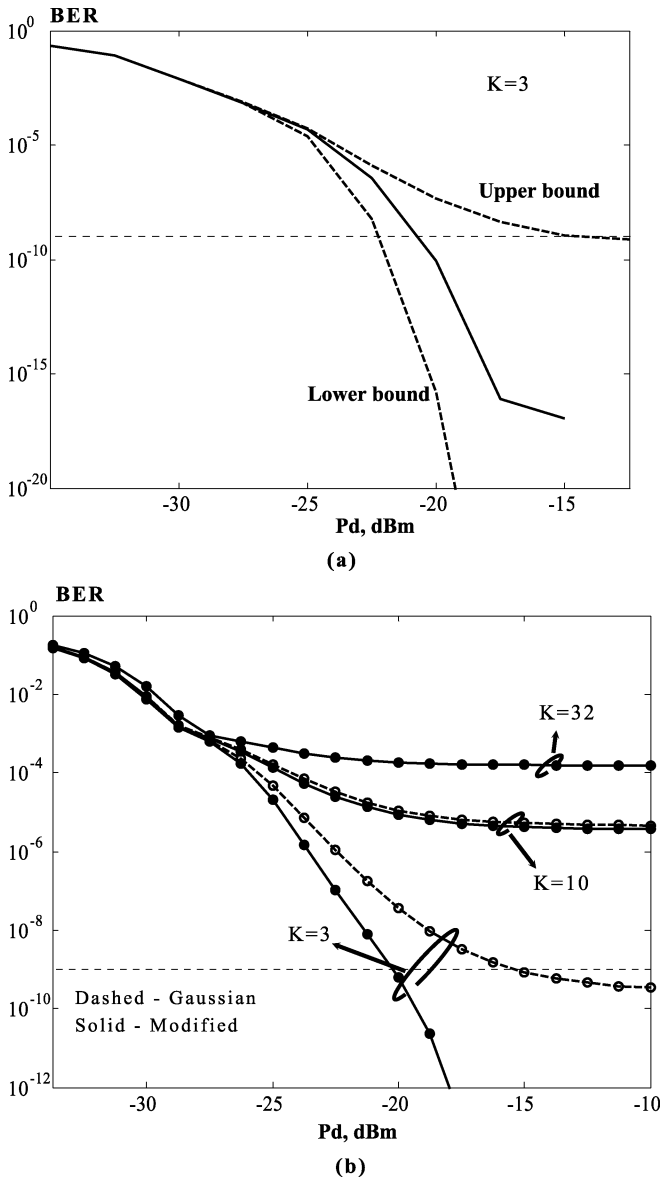

Fig. 3. BER performance evaluation using different noise pdfs (optimum threshold level D applied). (a) Upper and lower bound of the BER curve for $K = 3$. Upper bound: Gaussian pdf. Lower bound: Modified Gaussian pdf. Middle curve: Calculated using (12)–(14). (b) Upper and lower bounds of the BER performance for different K.

Thus, the error probability $Pe(0|1)(m)$ can be calculated using this modified Gaussian distribution and expressed as

$$Pe(0|1)(m) = \frac{1}{2}\left\{\text{erfc}\left[\frac{P_d(1+m\xi-D)}{\sqrt{2}\sigma_{1-\text{co}}}\right] + \text{erfc}\left[\frac{2m\sqrt{\xi}P_d}{\sqrt{2}\sigma_{1-\text{in}}}\right] - \text{erfc}\left[\frac{2m\sqrt{\xi}P_d}{\sqrt{2}\sigma_{1-\text{co}}}\right]\right\}, \quad \text{if } D > 1 + m\xi - 2m\sqrt{\xi}$$

$$Pe(0|1)(m) = \frac{1}{2}\text{erfc}\left[\frac{P_d(1+m\xi-D)}{\sqrt{2}\sigma_{1-\text{in}}}\right] \quad \text{others.} \tag{17b}$$

The noise pdfs calculated from these three expressions with different values of m are plotted in Fig. 2. The variations be-

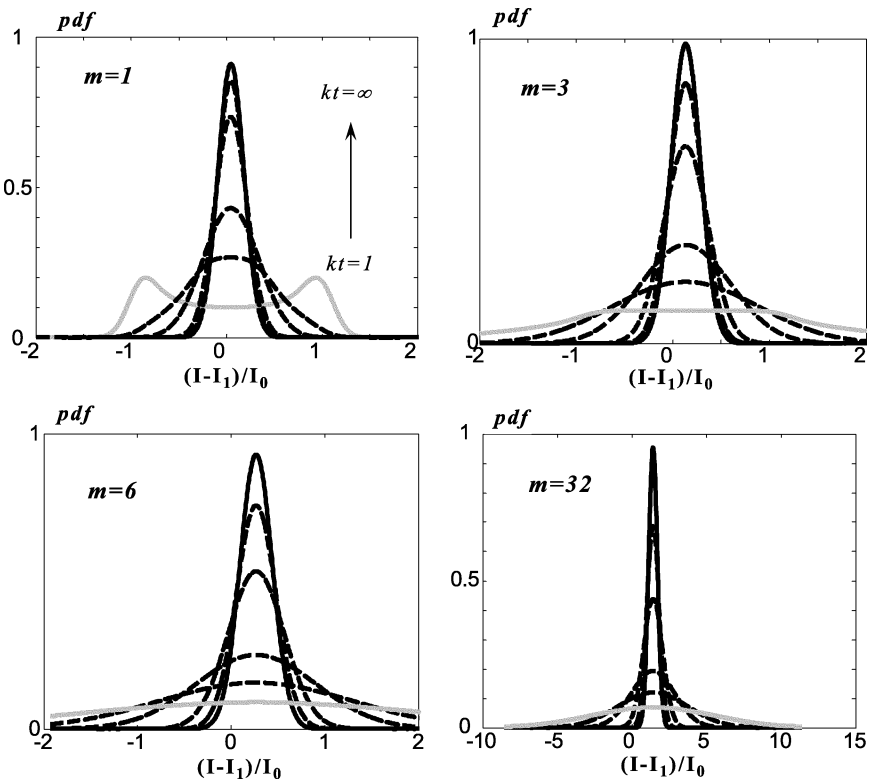

Fig. 4. Noise pdf with different values of kt for various m.

tween them are quite remarkable when m is low, but as m increases, the profiles become identical.

We also evaluated the BER performance using these pdf expressions for $K = 3$ [Fig. 3(a)]. The Gaussian pdf gives the *upper* bound of the system BER, while the modified Gaussian pdf gives the *lower* bound. Fig. 3(b) compares the results of the two approximations with different values of K. If K is large enough, the deviations between the approximations are negligible, but if $K < 5$, the difference is quite large. (In all these calculations, an optimal D value is applied to minimize the BER.)

C. Partially Coherent Regime $(kt > 1)$

Generally, the average received signal in the partially coherent regime is given also by (9). $P(1|0)(m)$ should also be the same as (10a) for the reasons given in case B.

The noise pdf with chip mark "1" can be derived from (5), as follows:

$$\text{pdf}(x,m) = F\left[M_p(\omega)\right] = \frac{1}{2\pi}\int_{-\infty}^{\infty} M_p(\omega)\exp(-j\omega x)d\omega \tag{18}$$

where

$$M_p(\omega) = \left\{ J_0^{\lfloor kt \rfloor}\left(\frac{2\sqrt{\xi}P_d\omega}{kt}\right)\cdot J_0\left(\left(1-\frac{\lfloor kt \rfloor}{kt}\right)2\sqrt{\xi}P_d\omega\right)\right\}^m \times\exp\left[-\frac{\sigma_1^2\omega^2}{2}\right]\exp\left[jm(\xi+\sqrt{\xi})P_d\omega\right]. \tag{19}$$

Here, $\lfloor kt \rfloor$ gives the integer part of number kt. The error probability $Pe(0|1)(m)$ can be obtained from (15). We can easily prove that when $kt = 1$, (19) becomes the same as (14); when $kt \to \infty$, (18) turns out to be a Gaussian distribution.

The noise distributions with different values of kt and a different number of interference signals m are plotted in Fig. 4. With the increase of kt, the noise pdf changes from the coherent limit $(kt = 1)$ to the incoherent limit $(kt \to \infty)$. This shows how the beat noise is eliminated from a system through an increase in the coherent ratio kt.

IV. Performance Limitations Due to the Beat Noise and the Means of Beat Noise Suppression

The effects of different noise sources on the BER performance of a TS-OCDMA system are illustrated in Fig. 5 (solid lines). In this example, $K = 32$, the lowest solid curve in the figure is with receiver noise only, the middle one is that of an incoherent network with receiver noise plus MAI noise, and the highest one is that of coherent TS-OCDMA with beat noise. We can see that the MAI noise is the dominant noise source in incoherent TS-OCDMA, while the beat noise dominates in coherent TS-OCDMA and thus is the main limit on system performance.

The dashed curves in Fig. 5 clearly show the relationship between the BER performance and the coherent ratio kt of the system. The impact of the beat noise in a TS-OCDMA network is highly dependent on the coherent ratio kt: from the coherent limit $(kt = 1)$, which is beat noise dominated, to the incoherent limit $(kt \to \infty)$, which is MAI-noise dominated, the impact of beat noise is gradually eliminated with increasing kt.

Fig. 6(a) shows the power penalty (at BER $= 1\times10^{-9}$) of the TS-OCDMA system with (coherent) and without (incoherent) beat noise versus K using 127-chip Gold code. Fig. 6(b) shows

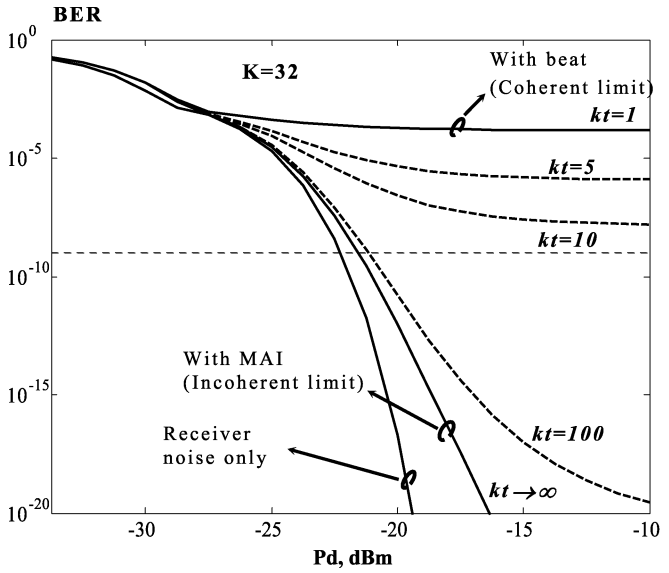

Fig. 5. Influence of the different noise sources and the coherent ratio kt on the BER performance of a TS-OCDMA network with 32 active users.

the power penalty versus the crosstalk level ξ for $K = 10$. The base line is that with the receiver noise only. The results of using two BER approximations are also plotted to show the upper and lower bounds. Fig. 6(a) shows that because of beat noise the coherent TS-OCDMA using 127-chip Gold code can only support five active users for error-free (10^{-9}) transmission, whereas, without beat noise, it can accommodate more than 40. Fig. 6(b) shows that to support ten active users for error-free transmission, ξ must be about -30 dB, which means the code length should be about 1000. That will be prohibitively large for practical encoder/decoder devices.

Three points need to be noted regarding these results. One is that in the above calculations, optimal threshold values *Dopt* are applied. The differences between the BER performance with *Dopt* and that using a fixed $D = 0.5$ can be seen in Fig. 7. The value of *Dopt* is determined by solving the equation $\partial(\text{BER})/\partial D = 0$ numerically (the curve with circles in the figure). The second point concerns the chip-rate detection in our model. In practice, chip-rate detection may not be available as the photodetector is not fast enough. The use of a PD with a narrower bandwidth B will result in a longer integration time in the model, thus degrading BER performance. Fig. 7 also shows the BER performance for different PD bandwidths. The third point is that in a 2-D OCDMA scheme with a coherent laser source, as in each wavelength, the signal is coherent time-spread, so it could be regarded as a partially coherent TS-OCDMA scheme with $kt \cong p_s$. Here, p_s is the weight of the encoded signal. In a symmetric 2-D OCDMA system $p_s = p_h$ (p_h is the number of available wavelengths) [18]–[25], [29]. Therefore, we can expect the degradation due to beat noise to also be eliminated if a large number of wavelengths are used.

As the beat noise critically limits system performance in coherent and partially coherent TS-OCDMA networks, a way to alleviate its impact is crucial in OCDMA networks. In Table I, we classify the means to suppress beat noise into three mechanisms and summarize several possible methods. The first mechanism is to reduce the crosstalk level (ξ). The use of longer code

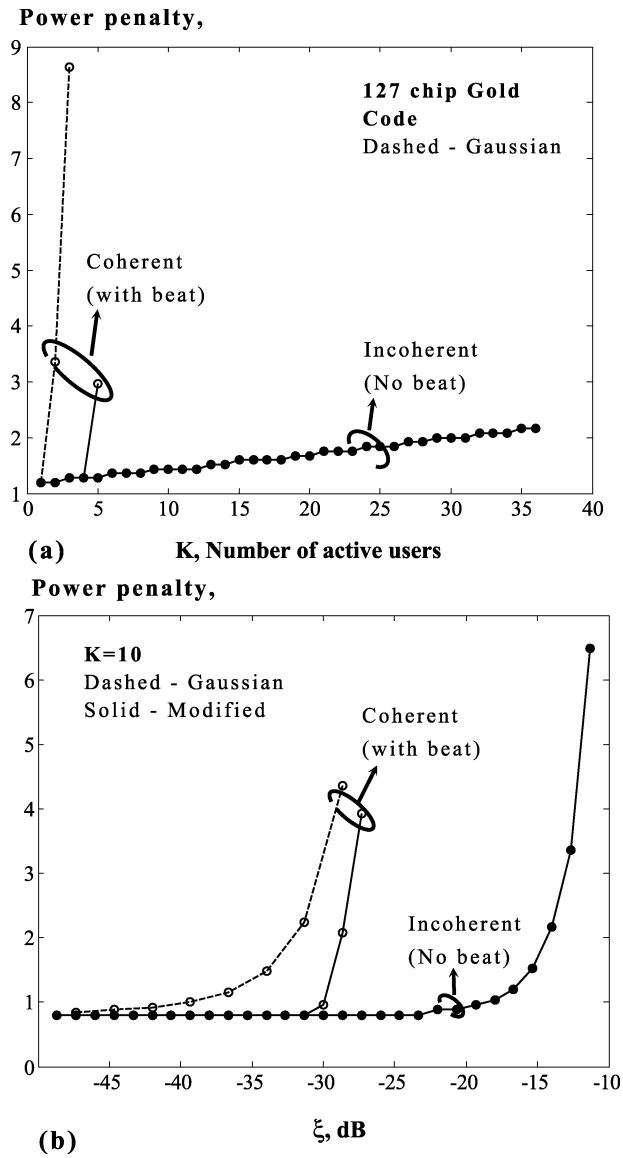

Fig. 6. Power penalty versus (a) K and (b) ξ for coherent and incoherent time-spreading OCDMA networks.

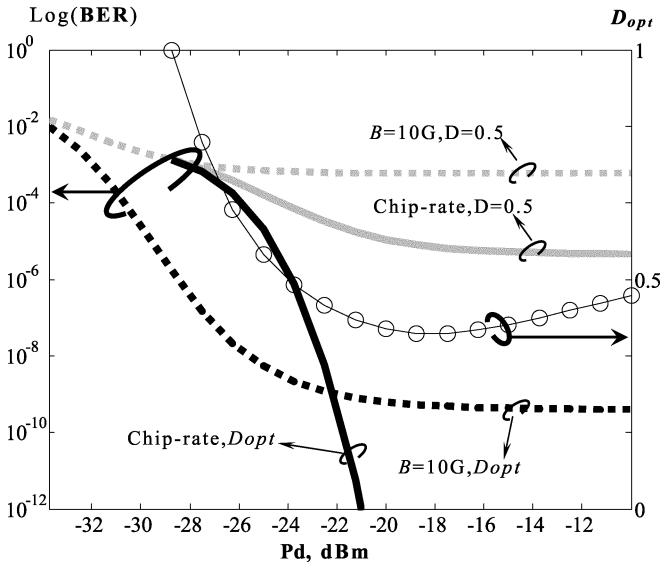

Fig. 7. BER performance with optimal (black line) and fixed (gray line) D, and under-chip-rate detection.

TABLE I
MEANS OF SUPPRESSING BEAT NOISE IN AN OCDMA-PON

Mechanism	Method	Notes	
		Partially coherent OCDMA	Coherent OCDMA
Reduce crosstalk	Using longer code	The code is too sparse, low power & bandwidth efficiency	Increased hardware cost & limited transmission data rate
	Synchronized OCDMA	1. Need control of optical path within chip-length (mm) order (for precise synch.) 2. Lowers the bandwidth efficiency (rough synch.)	
Polarization state	Polarization scrambling or modulation	Not effective for PON environment	
Low-coherence source	LED, ASE, chirped DFB, modulation, etc.	Effective because of increased *kt*	Not effective for the coherence required in a chip duration (Tc*B ~1)

is the most effective way to do this. This will lead to an increase of hardware cost and lower bandwidth efficiency. However, the progress made in SSFBG fabrication techniques has made it possible to produce ultralong optical codes with a very high chip rate [35]. Another way is to use a synchronized scheme. With a precisely synchronized scheme, ξ can be reduced to a reasonably low level. However, the system synchronization requirement is too strict to be realized in practical network environments. A roughly synchronized scheme can mitigate this problem by allowing the crosstalk from different users to offset each other, but this will lead to lower bandwidth efficiency.

The second mechanism is to control the polarization state of the crosstalk from each user through polarization scrambling or modulation. This is effective if the polarization state is known *a priori* and controllable but cannot work in the PON environment.

The third mechanism is to lower the coherence of the light source. This is effective for partially coherent systems because kt is increased. This method cannot be used for coherent systems, however, because the coherent coding operation requires that $Tc * B \sim 1 (kt \sim 1)$.

V. CONCLUSION

Generally, TS-OCDMA systems can be classified according to the coherent ratio kt into incoherent $(kt \rightarrow \infty)$, coherent $(kt = 1)$, and partially coherent $(kt > 1)$ systems. kt reflects the coherent property of the light during the chip duration. The coherent scheme that works with bipolar codes is more efficient and enables better system performance than the partially coherent and incoherent schemes that work with unipolar codes. In a coherent system, however, the beat noise is the dominant noise source and main limit on system performance. In partially coherent systems, the effect of beat noise is gradually eliminated as kt rises. An incoherent system is free of beat noise and MAI noise is the dominant noise source.

There are several ways to overcome the beat noise in a coherent or a partially coherent TS-OCDMA network. Using a low-coherence light source is effective in partially coherent systems since this increases kt. In coherent systems, the use of longer codes and some kind of synchronization scheme can lower crosstalk, thus mitigating the impairment of beat noise.

For the coherent TS-OCDMA PON, beat noise is a serious issue since it is the major limitation in network design. The recent progress made in SSFBG techniques shows that it is possible to eventually suppress the beat noise to an acceptable level in a coherent TS OCDMA network with an SSFBG encoder/decoder.

ACKNOWLEDGMENT

The authors would like to thank the anonymous reviewers for their careful reading and helpful comments. In addition, they thank K. Matsushima of Osaka University, Dr. S. Oshiba, and A. Nishiki of OKI Electric Industry Company, Ltd., for their invaluable discussions. In addition, X. Wang would like to thank the Telecommunication Advancement Research Fellowship of the Telecommunication Advancement Organization (TAO) of Japan.

REFERENCES

[1] P. R. Prucnal, M. A. Santoro, and T. R. Fan, "Spread spectrum fiber-optic local area network using optical processing," *J. Lightwave Technol.*, vol. 4, pp. 547–554, May 1986.

[2] J. A. Salihi and C. A. Brackett, "Code division multiple-access technique in optical fiber networks, part I: Fundamental principals and part II: Systems performance analysis," *IEEE. Trans. Commun.*, vol. 37, pp. 824–842, Aug. 1989.
[3] M. E. Marhic, "Trends in optical CDMA," in *Proc. Multigigabit Fiber Communication (SPIE)*, vol. 1787, 1992, pp. 80–98.
[4] D. D. Sampson, G. J. Pendock, and R. A. Griffin, "Photonic code-division multiple-access communications," *Fiber Integr. Opt.*, vol. 16, pp. 126–157, 1997.
[5] K. I. Kitayama, "Code division multiplexing lightwave networks based upon optical code conversion," *IEEE J. Select. Areas Commun.*, vol. 16, pp. 1209–1319, Sept. 1998.
[6] K. Kitayama, N. Wada, and H. Sotobayashi, "Architectural considerations of photonic IP router based upon optical code correlation," *J. Lightwave Technol.*, vol. 18, pp. 1834–1844, Dec. 2000.
[7] T. O'Farrell and S. I. Lochmann, "Performance analysis of an optical correlator receiver for SIK DS-CDMA communication systems networks with bipolar capacity," *Electron. Lett.*, vol. 30, pp. 63–65, 1994.
[8] L. Nguyen, T. Dennis, B. Aazhang, and J. F. Young, "Experimental demonstration of bipolar codes for optical spectral amplitude CDMA communication," *J. Lightwave Technol.*, vol. 15, pp. 1647–1673, Sept. 1997.
[9] C. F. Lam, D. T. K. Tong, M. C. Wu, and E. Yablonovitvh, "Experimental demonstration of bipolar optical CDMA system using a balanced transmitter and complementary spectral encoding," *IEEE Photon. Technol. Lett.*, vol. 10, pp. 1504–1506, Oct. 1998.
[10] E. D. J. Smith, R. J. Blaikei, and D. P. Taylor, "Performance enhancement of spectral-amplitude-coding optical CDMA using pulse-position modulation," *IEEE. Trans. Commun.*, vol. 46, pp. 1176–1185, Sept. 1998.
[11] R. A. Griffin, D. D. Sampson, and D. A. Jackson, "Coherence coding for photonic code-division multiple access networks," *J. Lightwave Technol.*, vol. 13, pp. 1826–1837, Sept. 1995.
[12] M. E. Maric, "Coherent optical CDMA networks," *J. Lightwave Technol.*, vol. 11, pp. 854–864, May 1993.
[13] N. Wada and K. Kitayama, "A 10 Gb/s optical code division multiplexing using 8-chip optical bipolar code and coherent detection," *J. Lightwave Technol.*, vol. 17, pp. 1758–1765, Oct. 1999.
[14] J. A. Salehi, A. M. Weiner, and J. P. Heritage, "Coherent ultrashort light pulse code-division multiple access communication systems," *J. Lightwave Technol.*, vol. 8, pp. 478–491, Mar. 1990.
[15] C. C. Chang, H. P. Sardesai, and A. M. Weiner, "Code-division multiple-access encoding and decoding of femtosecond optical pulses over a 2.5 Km fiber link," *IEEE Photon. Technol. Lett.*, vol. 10, pp. 171–173, Jan. 1998.
[16] H. Tsuda, H. Takenouchi, T. Ishii, K. Okamoto, T. Goh, K. Sato, A. Hirano, T. Kurokawa, and C. Amano, "Spectral encoding and decoding of 10 Gbit/s femtosecond pulses using high resolution arrayed-waveguide grating," *Electron. Lett.*, vol. 35, pp. 1186–1187, 1999.
[17] A. Grunnet-Jepsen, A. E. Johnson, E. S. Maniloff, T. W. Mossberg, M. J. Munroe, and J. N. Sweetser, "Fiber Bragg grating based spectral encoder/decoder for lightwave CDMA," *Electron. Lett.*, vol. 35, pp. 1096–1097, 1999.
[18] L. Tancevski, I. Andonovic, and J. Budin, "Massive optical LAN's using hybrid time spreading/wavelength hoping scheme," presented at the Integrated Optics Optical Fiber Communication (IOOC'95), Hong Kong, China, June, 26–30 1995, Paper TuA1-2.
[19] G. C. Yang and W. C. Kwong, "Performance comparison of the multiwavelength CDMA and WDMA+CDMA for fiber-optic networks," *IEEE. Trans. Commun.*, vol. 45, pp. 1426–1434, Nov. 1997.
[20] H. Fathallah, L. A. Rusch, and S. LaRochelle, "Passive optical fast frequency-hop CDMA communications system," *J. Lightwave Technol.*, vol. 17, pp. 397–405, Mar. 1999.
[21] X. Wang, K. T. Chan, Y. Liu, L. Zhang, and I. Bennion, "Novel temporal/spectral coding technique based on fiber Bragg gratings for fiber optic CDMA application," in *Dig. Optical Fiber Communication/Integrated Optics Optical Fiber Communication Conf. (OFC/IOOC'99)*, 1999, Paper WM50, pp. 341–343.
[22] N. Wada, H. Sotobayashi, and K. Kitayama, "2.5 Gbit/s time-spread/wavelength-hop optical code division multiplexing using fiber Bragg grating with super continuum light source," *Electron. Lett.*, vol. 36, pp. 815–817, 2000.
[23] S. Yegnanarayanan, A. S. Bhshan, and B. Jalali, "Fast wavelength-hopping time-spreading encoding/decoding for optical CDMA," *IEEE Photon. Technol. Lett.*, vol. 12, pp. 573–575, May 2000.
[24] K. Yum, J. Shin, and N. Park, "Wavelength-time spreading optical CDMA system using wavelength multiplexers and mirrors fiber delay lines," *IEEE Photon. Technol. Lett.*, vol. 12, pp. 1278–1280, Sept. 2000.
[25] X. Wang and K. T. Chan, "A sequentially self-seeded Fabry–Pérot laser for two-dimensional encoding/decoding of optical pulses," *IEEE J. Quantum Electron.*, vol. 39, pp. 83–90, Jan. 2003.
[26] P. C. Teh, P. Petropoulos, M. Ibsen, and D. J. Richardson, "A comparative study of the performance of seven- and 63-chip optical code-division multiple-access encoders and decoders based on superstructured fiber Bragg gratings," *J. Lightwave Technol.*, vol. 9, pp. 1352–1365, Sept. 2001.
[27] P. C. Teh, M. Ibsen, L. B. Fu, J. H. Lee, Z. Yusoff, and D. J. Richardson, "A 16-chnnel OCDMA system (4 OCDM × 4 WDM) based on 16-chip, 20 Gchip/s superstructure fiber Bragg gratings and DFB fiber laser transmitters," in *Proc. Optical Fiber Communication Conf. (OFC'2002)*, Los Angles, CA, ThEE1, pp. 600–601.
[28] Z. Wei, H. Ghafouri-Shiraz, and H. M. H. Shalaby, "New code families for fiber-Bragg-grating-based spectral-amplitude-coding optical CDMA systems," *IEEE Photon. Technol. Lett.*, vol. 13, pp. 890–892, Aug. 2001.
[29] L. Tančevski and L. A. Rusch, "Impact of the beat noise on the performance of 2-D optical CDMA systems," *IEEE Commun. Lett.*, vol. 4, pp. 264–266, Aug. 2000.
[30] P. J. Legg, M. Tur, and I. Andonovic, "Solution paths to limit interferometric noise induced performance degradation in ASK/direct detection lightwave networks," *J. Lightwave Technol.*, vol. 14, pp. 1943–1953, Sept. 1996.
[31] M. Tur and E. L. Goldstein, "Dependence of error rate on signal-to-noise-ratio in fiber-optic communication systems with phase-induced intensity noise," *J. Lightwave Technol.*, vol. 7, pp. 2055–2058, Dec. 1989.
[32] J. W. Goodman, *Statistic Optics*. New York: Wiley, 1985.
[33] X. Wang, K. I. Kitayama, and K. Matsushima, "Beat noise limitation in coherent time-spreading OCDMA network," in *Proc. 8th OptoElectronics Communication Conf. (OECC'2003)*, Shanghai, China, 2003, Paper 16E2-4, pp. 727–728.
[34] X. Wang, K. Matsushima, K. I. Kitayama, A. Nishiki, and S. Oshiba. Demonstration of the improvement of apodized 127-chip SSFBG in coherent time-spreading OCDMA network. presented at *Optical Fiber Communication Conf. (OFC'04)*. [CD-ROM] Paper MF74
[35] X. Wang, K. Matsushima, A. Nishiki, N. Wada, F. Kubota, and K.-I. Kitayama, "Experimental demonstration of 511-chip 640 Gchip/s superstructured FBG for high performance optical code processing," in *Proc. Eur. Conf. Optical Communication (ECOC'04)*, 2004, Paper Tu1.3.7, pp. 134–135.

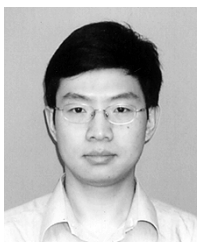

Xu Wang (M'02) received the B.S. degree in physics from Zhejiang University, Hangzhou, China, in 1989, the M.S. degree in electronic engineering from the University of Electronics Science and Technology of China (UESTC), Chengdu, China, in 1992, and the Ph.D. degree in electronic engineering from the Chinese University of Hong Kong (CUHK), Hong Kong, in 2001.

From 1992 to 1997, he was a Faculty Member and Lecturer in the National Key Laboratory of Fiber Optic Broad-Band Transmission and Communication Networks of UESTC. From 2001 to 2002, he was a Postdoctoral Research Fellow in the Department of Electronic Engineering of CUHK. He subsequently worked in the Department of Electronic and Information Systems of Osaka University, Osaka, Japan, as a TAO Research Fellow. In April 2004, he jointed the Ultra-fast Photonic Network Group of Information and Network Systems Department, National Institute of Communication and Information Technology (NICT), Tokyo, Japan, as an Expert Researcher. His research interests include fiber-optic communication networks, optical-code-division multiplexing, optical packet switching, semiconductor lasers, application of fiber gratings, and fiber-optic signal processing. He has authored approximately 40 technical papers in refereed journals and conferences.

Dr. Wang received the Telecommunications Advancement Research Fellowship by the TAO of Japan in 2002 and 2003.

Ken-ichi Kitayama (S'75–M'76–SM'89–F'02) received the B.E., M.E., and Dr.Eng. degrees in communication engineering from Osaka University, Osaka, Japan, in 1974, 1976, and 1981, respectively.

In 1976, he joined the NTT Electrical Communication Laboratory. He spent a year at the University of California, Berkley, as a Visiting Scholar from 1982 to 1983. In 1995, he joined the Communications Research Laboratory, Ministry of Posts and Telecommunications of Japan. Since 1999, he has been a Professor with the Department of Electronics and Information Systems, Graduate School of Engineering, Osaka University, Osaka, Japan. His research interests are in photonic networks and radio-on-fiber wireless communications. He has published more than 160 papers in refereed journals, and he has been awarded more than 30 patents.

Prof. Kitayama currently serves on the editorial boards of the IEEE PHOTONICS TECHNOLOGY LETTERS and IEEE TRANSACTIONS ON COMMUNICATIONS. He received the 1980 Young Engineer Award from the Institute of Electronic and Communications Engineers of Japan and the 1985 Paper Award of Optics from the Japan Society of Applied Physics. He is a Member of the Institute of Electronics, Information and Communication Engineers (IEICE) of Japan and the Japan Society of Applied Physics.